Organic & Biomolecular Chemistry

Accepted Manuscript

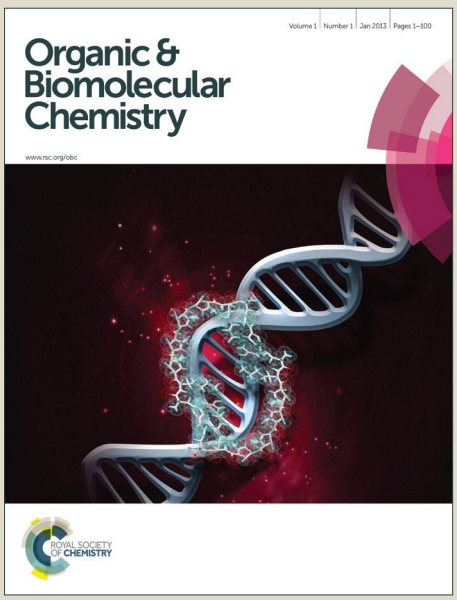

ROYAL SOCIETY OF CHEMISTRY

www.rsc.org/obc

Effective Chemiluminogenic Systems Based on Acridinium Esters Bearing Substituents of Various Electronic and Steric Properties†

Beata Zadykowicz[1], Justyna Czechowska[1], Agnieszka Ożóg[1], Anton Renkevich[2], Karol Krzymiński[1*]

[1] *Faculty of Chemistry, University of Gdańsk, Wita Stwosza 63 St., 80−308 Gdańsk, Poland*

[2] *Department of Chemical Metrology, Kharkiv V.N. Karazin National University, Kharkiv, 61022, Ukraine*

**corresponding author: karol.krzyminski@ug.edu.pl*

† Electronic supplementary information (ESI) available. See DOI:

Abstract

A series of 10-methyl-9-(phenoxycarbonyl)acridinium trifluoromethanesulfonates (XAEs), bearing substituents of various characteristics in the lateral benzene ring (2-halogen, 2,6-dihalogen, 2-trifluoromethyl, 2-nitro, 2-methoxy, 3-halogen and 4-halogen) were synthesized with high yields, identified and subjected to a physicochemical and theoretical investigation. The main task of the work was to assess the mechanism and optimal conditions of light emission in various liquid systems based on the above salts in order to evaluate their potential usefulness as chemiluminescence (CL) labels and indicators in an ultra-sensitive analyses. Density functional theory (DFT) calculations were performed to investigate the detailed mechanism of the oxidation of 9-substituted 10-methylacridinium cations involved in XAEs by hydrogen peroxide in alkaline media. Three general pathways were drawn, which are termed the "light path" (chemiluminogenic) and two "dark paths" (non-chemiluminogenic): hydrolytic and "pseudobase". The CL time profiles, triggered in alkaline solutions containing hydrogen peroxide, enabled us to establish crucial physicochemical parameters, including pseudo-first order kinetic constants of CL decay and relative efficiencies of emission. In order to optimize the systems' luminogenic performance, different bases, such as sodium hydroxide, tetrabutylammonium hydroxide (TBAOH) and 1,8-diazabicyclo[5.4.0]undec-7-ene (DBU), as well as enhancers, such as cationic, zwitterionic and neutral surfactants (cetyltrimethylammonium chloride, (CTAC), N,N-dimethyldodecylammonio-1,3-propane sulfonate (DDAPS) and Triton X-100,

respectively) were tested. The results revealed the optimal CL systems, which enabled us to obtain substantially higher emissions than typical ones, based on acridinium esters or luminol. The derived parameters, characterizing the potential utility of the acridinium esters, such as stability in aqueous environments and usefulness (the product of emission efficiency and stability at given pH), enabled us to reveal the best candidates and their practical applications. The post-reaction mixtures, analyzed by means of chromatography (RP-HPLC) and mass spectrometry (ESI-MS), allowed us to verify the occurrence and population of the products, that were theoretically predicted, i.e. 10-methyl-9-acridinone (NMAON), 10-methylacridinium-9-carboxylic acid (NMACA) and substituted phenols (RPhOHs).

Introduction

Chemiluminogenic acridinium esters (AE), first described by F. McCapra in the 1960s, were introduced to medical diagnostics about twenty years later.[1,2] In contrast to the commonly employed phthalic acid hydrazides, they do not require the use of a catalyst to trigger CL and, in general, are characterized by a high temporary intensity of emission − up to 100-fold higher than luminol.[3] The quantum yield of most AEs are at the level of 2% in aqueous environments, which can be considered a high value compared to luminol (ϕ_{CL} = 1.23%, the standard used in luminometric assays[4]) enabling the direct quantification of the analyte in a given system at the femtomolar or even lower level of concentrations.[5,6] The carrier of AEs and some other quaternary acridinium salts (9-sulphonamides, 9-cyanides) in modern analysis is also determined by the possibility of their relatively easy chemical modifications and the simplicity of the CL assays.[7,8] Today, applications of AEs cover a wide area of immunodiagnostics, where they are used in a chemically bound form (CL labels)[8], as well as environmental analyses – where they are utilized in the free form (CL indicators).[6,9] Acridinium labels and indicators have been employed, among others, for assaying human α-fetoprotein, gonadotropins, thyroid stimulating hormone (TSH), viruses, markers of cancer cells, nucleic acids, oxidative enzymes (e.g. glucose oxidase, horseradish peroxidase) and other important bioanalytes.[1−3,8,10,11] AEs were also utilized to determine the trace amounts of environmental pollutants, such as hydrogen peroxide or substituted phenols.[3,12] Recently, acridinium salts were employed in serial clinical assays performed with the aid of automated clinical analyzers – such as Abbott Prism® or Siemens Advia Centaur® – in the routine monitoring of blood quality for the presence of HBC, HCV, HIV-1, HIV-2 and other viruses.[10] Other examples of diagnostic methods developed with the participation of AEs are

affinity tests, applied in the investigation of nucleic acids (also in automated variants).[13,14] The latter approach makes an alternative for DNA sequencing, gel electrophoresis, mass spectrometry and other techniques employed in nucleic acid chemistry. Recently, new variants of nucleic acid hybridization AE-based tests, with no need for their amplification, were proposed.[15,16] The introduction of the electron-donating alkoxy substituents (e.g. OCH_3) into the conjugated ring system of AE resulted in a shift of the emission range towards longer wavelengths, and a slight enhancement of its efficiency.[16,17] The authors also stated that the introduction into the benzene ring electron-withdrawing Br atoms (ortho positions) of AE enables the trigger of the ring efficient emission at relatively low pH values (pH = 9). The proposed design of new AE labels should guarantee their increased resistance to hydrolysis and good dynamics of light emission (which finally enables lower limits of detection). Other studies on variously substituted acridinium esters indicated that the introduction of oxygen-rich groups (such as polyethylene glycol (PEG) residues or alkylsulfopropyl groups) and bulky polar substitutents (such as Br) into specific locations of the aromatic ring systems results in a substantial increase in the luminogenic capability of the respective compounds (up to four times).[18–21] The polar groups improve the solubility of the related derivatives and, presumably, help to reduce their hydrophobic aggregation after conjugation with the bioanalyte accompanied with low non-specific binding.

Our previous investigations on the CL of AEs were focused on the family of alkylphenyl esters of 10-methylacridinium-9-carboxylic acids – molecular systems frequently incorporated in commercially available CL labels.[22,23] Experimentally established values − CL decay kinetic constants and integral efficiency of emission – showed correlations with the theoretically predicted parameters, such as activation barriers and specified geometrical parameters of the molecular systems involved in the light-emitting step. The presence of bulky alkyl substituents at the ortho- positions of the benzene ring drastically decreased the reaction course; their slight electron-donating character is manifested by the same effect, but more subtle. Among the interdependences revealed within this family of CL systems was the correlation between the AE's emission intensity and the volume of hydration layer of the leaving group[22] during the light-generating step. The latter important observation for the rational design of new acridine-based labels and indicators.

Natrajan's group determined the influence of various types of surfactants on the behavior of zwitterionic and alkyl-substituted AE labels and their protein conjugates.[24]

To take a deeper look at the physicochemistry and luminogenic properties of the AEs, we have synthesized a series of chemiluminogenic salts, differing in terms of the location and

the electronic and steric properties of the substituent(s) introduced into the lateral benzene ring (XAEs). In the past, we performed studies on the crystalline structures of XAEs, applying X-Ray crystallography methods, as they demonstrate interesting features in the solid phase.[25–31] On the other hand, applying differential scanning calorimetry methods to study their thermal behavior enabled us to assess important physicochemical parameters – such as the crystal lattice energy, enthalpies of volatilization and formation and others.[32]

In this work, we present investigations of the luminogenic properties of XAEs, including theoretical, structural and physicochemical studies in the liquid phase. Since most of the compounds presented here express higher emission efficiencies than their alkyl analogues[22], we attempt to reveal the possible reason(s) for this phenomenon, including analyses of the post-CL reaction mixtures. Within this work we also took under consideration the emission properties and crucial analytical parameters of XAEs in systems containing cationic, zwitterionic or neutral surfactants, being employed as CL enhancers in that context.[24] In order to understand the observed differences in physicochemical features, we applied computational methods based on Density Functional Theory (DFT), which enabled us to reveal the thermodynamic and kinetics parameters and to propose possible reaction pathways of chemiluminogenic oxidation of XAEs in various alkaline environments.

Results and discussion

Origin of chemiluminescence

Previous investigations by ourselves[22] and others[8,33] on the mechanism of the oxidation of 9-substituted 10-methylacridinium cations by H_2O_2 in alkaline media indicated that the primary steps of the reaction of XAEs with either OOH^- or OH^- are mainly determined by the location of the electrophilic center in the cation. According to the frontier orbital theory,[34] the Lowest Unoccupied Molecular Orbital (LUMO) distribution of an electrophilic species determines the molecular center sensitive to nucleophilic attack. The value of the LCAO coefficient of the p_z atomic orbital in the XAEs' LUMO is ca. 10 times higher at the endocyclic C(9) than at the C(15) carbonyl atom (0.30 and 0.03, respectively; average for **2-F**, **2-CF_3**, **2-NO_2**, **2-OCH_3** and **2,6-diBr**) (Scheme 1). This implies that C(9) rather than the C(15) marks the site of the primary nucleophilic attack of the above-mentioned anions, despite the fact that the Mulliken partial charge at C(9) is lower than at the C(15) atom of the carbonyl group (0.09 and 0.52, respectively; average for **2-F**, **2-CF_3**, **2-NO_2**, **2-OCH_3** and **2,6-diBr**). Another premise that must be taken into account is the fact that H_2O_2 reacts

spontaneously with OH^- to yield OOH^- (the thermodynamic data for the reaction $H_2O_2 + OH^- = H_2O + OOH^-$ are: –26.8, –27.9 and –20.6 kcal/mol (enthalpy (gaseous phase), Gibbs' free energy (gaseous phase) and Gibbs' free energy (aqueous phase) of the reaction at temperature 298.15 K and standard pressure, respectively).

Taking into account the reaction pathways proposed by other authors[8,33] and our previous investigations,[22] as well as the information mentioned above, we considered the processes in accordance with general chemical knowledge that may explain the experimental findings. The pathways of the possible reactions of XAEs with OOH^- and OH^-, outlined in Scheme 2, emerge from a thorough analysis of the results of theoretical calculations. Scheme 2 presents the processes that account for the CL (pathway one; steps I, VI, and VII; or I, XVI and XVIII), the formation of the so-called "pseudobase" (step II), and following non-CL processes (pathway two; steps IX and X; or XI, XII and XIII), the appearance of 10-methylacridinium-9-carboxylate anions or 10-methylacridinium carboxylic acid (pathway three; steps IV and XV, and step V, respectively) among the reaction products. The theoretically predicted thermodynamic data for all the reaction steps are given in Table 1, while Table 2 contains kinetic data for the steps involving molecules in the ground electronic state. Additionally, the DFT-optimized geometries originating from the acridine molecules produced by the reaction of XAEs with OOH^- or OH^- are shown in Figure S1† (lowest energy and transition state structures) in the Electronic Supplementary Information (ESI).

Pathway one ("light pathway") represents the attack of OOH^- on the XAE's acridinium carbon atom (9) (step I), followed by the reaction of the addition product **a** with OH^- (step VI), the cyclization of the anion to cyclic intermediate (**b**) (step VI), and the elimination of phenyl carbonate anion leading to the energy-rich 10-methyl-9-acridinone (**c**) (step VII). Interestingly, in the case of cations involved in **2-NO_2** and **2,6-diBr** (Scheme 1), we did not observe steps VI and VII. After the attack of OOH^- on the carbon atom C(9) of **2-NO_2** or **2,6-diBr** cation (step I), followed by the reaction of the addition product **a** with OH^- (step VI), the elimination of the adequate phenoxy anion and resultant cyclic intermediate (**e**) (step XVI) with the subsequent elimination of carbon dioxide leads to the energy-rich 10-methyl-9-acridinone (**c**) (step XVIII). We examined the two pathways (steps I, VI and VII; and I, XVI and XVIII) for compounds **2-F**, **2-CF_3** and **2-OCH_3**. The theoretically predicted thermodynamic data indicated that these two pathways are possible for compounds **2-F**, **2-CF_3** and **2-OCH_3**. On the other hand, the enthalpy (gaseous phase), Gibbs' free energy (gaseous phase) and Gibbs' free energy (aqueous phase) of step XVI (298.15 K, standard

pressure) are thermodynamically more preferred in the case of compounds **2-NO$_2$** and **2,6-diBr** than **2-F**, **2-CF$_3$** and **2-OCH$_3$**. The barriers predicted for step XVIII are similar in the aqueous phase to the barriers predicted for step VII (e.g. for compound **2-F** $\Delta_{a,298}G^o$ in the aqueous phase (in kcal mol^{-1}) are 15.4 and 14.1, respectively). The computationally predicted pathways of CL generation do not clearly present which pathway operates for the cations involved in **2-F**, **2-CF$_3$** and **2-OCH$_3$**. Just one thermodynamically possible pathway was observed in the case of XAEs, where the elimination of phenoxy anions after addition product **a** with OH^- (step VI) and formation of the cyclic intermediate **e** occur. The energy released in step VII or XVIII (Table 1) exceeds that necessary to cause the electronic excitation of 10-methyl-9-acridinone, which is 88.2 kcal mol^{-1}.[35]

Pathway two ("dark pathway") assumes the attack of OH^- on the XAE's carbon atom (9) (step II), followed by the reaction of the addition product **f** ('pseudobase') with OH^- (step IX) and the elimination of adequate phenoxy anion and carbon monoxide, leading to the 10-methyl-9-acridinone (**c**) (step X). Alternatively, the reaction of the addition product **f** ('pseudobase') through the attack of OOH^- on the carbon atom C(15) of the carbonyl group of the XAE (step XI), followed by elimination of a phenoxy anion leads to intermediate **i** (step XII), and the further elimination of carbon dioxide and water leads to 10-methyl-9-acridinone (**c**) (step XIII). The theoretically predicted thermodynamic data indicated that these pathways are possible for all of the investigated compounds. The enthalpy (gaseous phase), Gibbs' free energy (gaseous phase) and Gibbs' free energy (aqueous phase) computed at temperature 298.15 K and standard pressure suggest that the addition of OH^- to the C(9) (step II) is thermodynamically preferred over the addition of OOH^- to the same carbon atom. In this case, the possible pathway of reaction seems to be exclusively dependent on the kinetic factors. We noted earlier,[22] and have confirmed in our present calculations, that the activation barriers characterizing the addition of OOH^- or OH^- to C(9) of the acridinium esters (steps I and II, respectively) and the substitution at OOH^- of the carbonyl C(15) atom of the 'pseudobase', followed by the release of the phenoxy anion (steps XI and XII, respectively) are negligible. Activation barriers do, however, exist for the final steps (X and XIII), characterizing the transformation of XAE pseudobase form to 10-methyl-9-acridinone (Table 2). In the case of step X, the activation barriers fall in the range of 5–14 kcal mol^{-1}, which are comparable to the activation barriers characterizing step VII. Nevertheless, the energy released is too small to electronically excite the above product (Gibbs' free energy in the aqueous phase are between –30 to –47 kcal mol^{-1}) (Table 1). The overall values of the

thermodynamic functions for step XIII (Table 1) are high enough to ensure electronic excitation of the produced 10-methyl-9-acridinone, but the activation barrier characterizing this process is significantly higher than that of steps VII or X (Table 2). For the above reasons, pathway two, assuming the attack of OH^- on XAEs' C(9) cannot lead to CL and represents the dark transformation of XAE cations, producing 10-methyl-9-acridinone in the ground electronic state.

Pathway three explains the occurrence of 10-methylacridinium-9-carboxylate anions or 10-methylacridinium 9-carboxylic acid (steps IV and XV, and step V, respectively) among the reaction products, as OH^- – like OOH^- – can attack the acridinic carbon atom (9) or carbonyl carbon atom (15). The addition of OH^- to C(9) (pathway two) is more probable for the reasons mentioned above. As we noted earlier,[22] the identified entities were 10-methyl-9-acridinone (NMAON), 10-methylacridinium 9-carboxylic acid (NMACA) and substituted phenols (RPhOHs). The latter acid or its zwitterionic form, 10-methylacridinium-9-carboxylate, is likely formed as the result of XAEs' hydrolysis, which assumes the attack of OH^- on the carbonyl carbon C(15) (step IV), followed by the reaction of the addition product **j** with OH^- (step XV), and the elimination of adequate phenoxy anion and water molecule, leading to product (**k**). These two steps are possible only for the two species – 9-[(2-fluorophenoxy)carbonyl]-10-methylacridinium (**2-F**) and 9-[(2-methoxyphenoxy)-carbonyl]-10-methylacridinium (**2-OCH_3**) cations. In other cases (**2-CF_3**, **2-NO_2** and **2,6-diBr**), these steps presumably do not occur and NMACA is produced upon the attack of OH^- on the carbonyl carbon atom C(15) (step V), followed by simultaneous elimination of substituted phenoxy anion leading to product (**l**). The thermodynamic data (Table 1) indicate that this step is possible for all the theoretically investigated compounds, that are **2-F**, **2-CF_3**, **2-NO_2**, **2-OCH_3** and **2,6-diBr**. In the case of step V the alkaline hydrolysis of acridinium esters occurs with the formation of tetrahedral intermediate, which immediately decays into products (**l**) and substituted phenoxy anion. The activation barriers characterizing the addition of OOH^- to C(15) atom and formation of tetrahedral transition state are negligible (0.6 kcal mol^{-1}; average value for **2-CF_3**, **2-NO_2** and **2,6-diBr**). In our opinion more preferred pathway is that via the steps IV and XV, but the theoretically predicted data indicated that the latter pathway is not possible in the case of **2-CF_3**, **2-NO_2** and **2,6-diBr.**

Synthetic considerations

Although the methods for the preparation of 10-substituted 9-(phenoxycarbonyl)acridinium salts have been described in the literature,[22,25-32,36] a few remarks concerning the compounds investigated here should be mentioned (their synthesis and spectroscopic analyses are reported in ESI). To ensure a clean and effective synthesis of XAEs (Scheme 1), their immediate precursors, substituted 9-[(phenoxy)carbonyl]acridines, must be obtained in high yield and purity. According to this, we promptly chromatographed the reaction mixtures after the completion of the reaction, omitting numerous washings of the organic post-reaction mixture with aqueous solutions, that lower the yield of reaction.[22] The procedure is especially important if the sterically hindered phenols are used for esterification or the product contains hydrophilic atoms or group of atoms. TLC tests of the chromatographically (LC) purified (9-[(phenoxy)carbonyl]acridines showed no other residual acridines by fluorescence detection; however, the elemental analyses were not always satisfactory. Further investigation revealed that the residual impurities in the chromatographed materials arose from residual phenols, characterized by similar polarity as the uncharged esters. However, such impurities do not affect the quality of the final products (XAEs) – as phenols are washed away during the last step reaction (quaternization). If needed, the residual phenols can be easily removed from the final products by heating the products in a vacuum to about 100˚C – under such conditions their sublimation/evaporation take place.

The other important synthetic issue, that must be remarked on the reaction of the above-described esters with methyl triflate, is the special treatment of the solvent before the reaction (chloroform should be passed through a dried, basic Al_2O_3 column), as well as the need for the use of a "proton sponge" (such as immobilized 2,6-di-*tert*-butylpyridine) – in order to remove the acidic impurities from the reaction mixtures, greatly reducing the yield and quality of obtained salts. It must also be noted that, among other XAEs, the compound encoded **2,6-diI** (Scheme 1) caused experimental difficulties as it expressed limited photochemical stability, which was observed during the experiments.

Spectroscopic Properties of XAEs

According to ^{1}H and ^{13}C NMR techniques, that were employed for the identification of cations involved in XAEs, the compatibility of the experimental and computational chemical shifts was satisfactory as denoted by the data collected in Tables S1†−S3† and illustrated in Figure S2† (ESI).

In general, the ^{1}H NMR spectra of XAEs can be subdivided into three groups of signals[37] – those arising from the hydrogen atoms bonded to the acridine/acridnium nuclei (maximum range of chemical shifts, σ), the hydrogens present in the benzene ring (an intermediate range of σ), and – if present – the signals rising from the aliphatic hydrogen atoms (the lowest range of σ). In the group of 9-[(phenoxy)carbonyl]acridines (the unmethylated precursors of XAEs), the ^{1}H signals from the acridine nucleus H1/H8 and H4/H5 occur always at higher values of chemical shifts than H2/H7 and H3/H6 (Figure S2†, ESI). The latter observation is likely related to the "uncover" effect, applied by the carbonyl oxygen atom (in the case of H1/H8) or the endocyclic nitrogen atom (in the case of H4/H5). Due to their spatial proximity, the H1/H8 signals also seem to be the most sensitive to the substitution type in the benzene ring. The ^{1}H NMR spectra of XAEs are similar to the spectra of their precursors (The synthesis of XAEs, ESI). In these cases, the signals rising from the acridinium nucleus appear at higher value chemical shifts than the respective signals for the bases – due to the lowering of the electron density, especially in a spatial area close to the endocyclic nitrogen atom. The coupling constants, characterizing the direct vicinal protons in the XAEs, appear in a range of values characteristic for aromatic molecular systems (7.0–10.0 Hz). In the case of the couplings of higher orders, the values are located in the range of 0.5–2.5 Hz and reflect the individual features of the analyzed molecular systems. The ^{13}C NMR spectra of XAEs (Figure S2†, ESI) express typical pattern, characteristic for phenyl-substituted acridinium esters.[37] Each of the observed signal was attributed to the respective carbon atom (Table S2†, ESI) with the aid of HETCOR ^{1}H–^{13}C HSQC two-dimensional NMR spectra and the ACD/CNMR database.[55]

The data concerning cations involved in XAEs disclosed by mass spectrometry are summarized in Table S1† (columns 1–3 from right, ESI) and the representative MALDI-TOF spectra are presented in Figure S2† (ESI). In all cases, the mass spectra present a simple and clear pattern, underlining the chemical identity of obtained acridinium salts. The parent ions M^{+} or $(M+1)^{+}/(M-1)^{+}$ are observed with the relative abundances of 18–100% and 8–76%, respectively and the characteristic signal for all spectra – 10-methylacridinium cation ($MeAcr^{+}$, $m/z \approx 193$, or $(MeAcr^{+}+1)^{+}$, $(MeAcr^{+}-1)^{+}$ signals) – are observed within relative abundances of 21–100%.

Chemiluminogenic properties of XAEs

Kinetics of CL decay in various environments

The group of presently studied acridinium esters (XAEs) contain substituents of various electronic and steric character in the ester moiety (the leaving group during their chemiluminogenic oxidation) located at the *ortho*, *para* or *meta* positions of the benzene ring (Scheme 1). These substituents are electron-acceptor halogen atoms, nitro (NO_2) and trifluoromethyl (CF_3) and methoxy group (OCH_3), expressing an electron-donor character.[17,32]

As shown by the data presented in Figure 1, Figure 2A and summarized in Table S4†, column 2, ESI), an emission decays for most haloester salts, initiated by standard triggering reagents (H_2O_2/NaOH), represent high-speed (flash type) kinetics, with k_{CL} values falling in the range of ca. 3–5 s^{-1}. Thus, the investigated systems are characterized by emissions occurring on a time order of seconds as shown in an exemplary CL time profile for a series of 2-substituted XAEs (Figure 1). The behavior of the salts **2-NO_2** and **2-CF_3** are similar to the other 2-substituted haloesters. However, the compound bearing an electron-donor substituent (**2-OCH_3**) behaves differently in this context, exhibiting a glow-type emission ($k_{CL} \approx 0.4$ s^{-1}), typical for the majority of previously studied acridinium alkylesters.[17,32,38] Interestingly, the influence of the steric hindrance of substituents on k_{CL} it not clearly observed, if one compares the k_{CL} values, e.g. for compounds **2-F**/**2,6-diF** or **2 Br**/**2,6-diBr** (Figure 2A, Table S4†, ESI). The latter behavior differentiates XAEs (instead of **2-OCH_3**) from the above-mentioned alkylesters, where the spatial effect caused by the *ortho*-susbtitutents is distinct.[21,39] The use of organic bases instead of NaOH – such as sterically hindered tetrabutylammonium hydroxide (TBAOH) or a strong Lewis base, 1,8-diazabicyclo[5.4.0]undec-7-ene (DBU) in aqueous or methanolic environments was tested in order to examine how it affects the kinetics and efficiency of CL. We assumed that, with the use of other bases, the susceptibility of XAEs to the production of undesirable "pseudobases", as well as the mobility of the ions engaged in the reaction, might be altered. When using TBAOH, a clear acceleration of the emission dynamics was observed if compared to the situation when a typical triggers were used – by 20–50% in aqueous and by 50–80% in methanolic environments (Fig. 2A; Table S4†, columns 3 and 5). In turn, the use of DBU is, in general, manifested by a decrease of k_{CL} values by about 10–40% (Fig. 2A; Table S4†, column 4, ESI). Such observations may be associated with a lower degree of H_2O_2 ionization in the environment when DBU was used instead of the typical Brönsted bases. In addition, OH^- ions also act as a catalyst in stage VI of light-generating transformations (Scheme 2). Another observation, which might be

annotated, is that the properties of the environment (the base, solvent) express a more pronounced influence on the emission kinetics in the group of 2,6-disubstituted than 2-substituted XAEs (Fig. 2A).

Emission efficiency in various environments

The normalized values of the relative efficiencies of XAEs' emmision (*RCLE*) are compared in Figure 2B and summarized in Table S4† (columns 6–9, ESI). One can observe that, among the various compounds investigated, the differences in *RCLE* are not substantial, as was observed in the case of the above-discussed values of k_{CL}. However, if one takes into consideration the values of this parameters in various environments, the differences are more distinct.

Generally, the highest values of *RCLE* are obtained in TBAOH/H_2O, while the lowest values are obtained in the TBAOH/CH_3OH environment; the typical aqueous environment (NaOH/H_2O) is characterized by moderate efficiency – located in between the two former ones. Comparing the two graphs presented in Fig. 2 (A and B), it can be concluded that, in aqueous systems, a faster emission is generally accompanied by a higher efficiency. To some extent, this observation might be explained in terms of various amounts of 10-methylacridinium-9-carboxylic acid (NMACA), detected among CL reaction products.[22] The latter finding indicates various participation of the hydrolytic dark paths IV and V (Scheme 2) among the reaction pathways. This problem will be further discussed below (The products secreted upon XAEs' chemiluminescence). On the other hand – faster kinetics in methanol is not accompanied by a higher efficiency emission of XAEs – as RCLEs characterizing the TBAOH/MeOH system take the lowest values (instead of **2-OCH$_3$**, Fig. 2B, Table S4† (ESI)). The circumstances, whose importance is hard to estimate just on the basis of CL measurements – such as an altered mechanism of light generation in an organic environment or different excitation efficiency of the oxidation product – might be considered to explain that observation.

The values of quantum yields (QY) determined for XAEs, using luminol as a reference,[22] are collected in column 10 of Table S4† (ESI). Generally, slightly higher emission yields for XAEs than for the previously investigated acridinium alkylesters in alkaline aqueous environment (NaOH/H_2O) can be noted.[22] In this context, the fluorinated derivatives are characterized by maximal QY values in the group of investigated salts, e.g. 2.3–2.4% in the case of **2-F** and **3-F** – which is more than 25% higher than those obtained for the unsubstituted AE in the same environment.

Alkalinity of environment's vs CL efficiency

As regards the influence of the environment's pH on the emission efficiency (*RCLE*) in the group of XAEs, the information obtained from CL measurements are compared in Fig. 3A and summarized in Table S4† (columns 11–13, ESI). In general, a lower pH of the CL environment is manifested by a substantial reduction in *RCLE* values. This behavior is likely accompanied from a lower population of OOH^- ions (pK_a of H_2O_2 = 11.75)[41] in solutions of lower alkalinity. The decrease in efficiency is irregular – a change of pH from 12 to 10 leads to a slight (few percent) reduction in the *RCLE* (as it takes place in the case of 2- and 4-substituted XAEs), whereas a further lowering of the pH value (pH = 8) is manifested in a substantial reduction of emission efficiency (up to several dozen percent). In the case of **2-OCH$_3$** the emission practically disappears at pH = 8. However, some XAEs retain their emission ability at pH = 8 reasonably well (about 50% of the original value) – such as compounds **2,6-diF** and **2-NO$_2$**. The latter effect is likely associated with their substituent-driven activation towards nucleophile attack (OOH^-) onto the C(9) atom, starting the "light pathway" of oxidation of XAEs (Scheme 2 , pathway I).

Other parameters characterizing XAEs' emission ability

The last column in Table S4† (ESI) contains parameters named stability, reflecting the degree of the retained XAEs' emission activity after incubation in alkaline phosphate buffer (pH = 8.0, *t* = 30 min., T = 298 K). This parameter seems to be important in the context of the utilization of XAEs as fragments of CL labels – where the covalent attachment of a label to a biomolecule requires the incubation of the ester in the above-mentioned conditions.[8] As revealed from the data presented in Table S4†, the stability of most XAEs fluctuates around 50%, although some compounds (**2-OCH$_3$**, **2,6-diBr**) retain more than 70% of their emission ability under experimental conditions. The possible reasons for this might be considered in the context of the electronic and steric influence of the substituents that are present in the benzene ring. In the group of 2,6-dihaloesters, the trend is towards strengthening the compounds' stability in the order: **2,6-diBr** > **2,6-diCl** > **2,6-diF**. The least stable compound, that is **2-NO$_2$**, loses ca. 75% of its emission ability under the same conditions – apparently because of the strong susceptibility to alkaline hydrolysis.

Interesting conclusions can be drawn from the chart, presenting "usefulness" of XAEs (Fig. 3B). Usefulness is the original parameter, which we have proposed previously,[22] being the product of emission efficiency at a given pH (12 or 8) and the stability in an alkaline environment (pH = 8). It can be employed – among other physicochemical characteristics,

such as kinetics of emission, thermodynamic stability – as a measure of potential utility of a given compound as a CL label or indicator. According to this, the compounds that are intended to be used as CL labels should be characterized by high usefulness at high pH values – under which the emission of the labeled conjugates is triggered. Accordingly, mono-fluorinated compounds, such as **3-F**, **2-F**, **4-F** or **4-Br** and **2-OCH$_3$**, seem to be particularly useful in this context (Fig. 3B, dark bars). On the other hand, if relatively low alkalinity, at which the emission is triggered is important – which, for example, takes place in nucleic acid diagnostics or CL ELISA applications (where AEs are used as CL indicators) – obtaining a high usefulness of CL reagents at pH = 8 would be beneficial. In this context, the XAEs containing two halogen atoms in both ortho-positions – in particular the compound **2,6-diF** (Fig. 3B, light bars) – would be beneficial.

The previously reported trend among acridinium chemiluminogenic salts indicated that, in general, the dynamics of light emission increases as the pK_a of the leaving group decreases, i.e. the moiety detached upon CL becomes a "better" leaving group.[42] In the present work we were unable to observe a clear relationship between kinetics or efficiency and pK_a of the respective phenol among all the investigated XAEs. However, in the sub-group of the salts with no steric hindrance, i.e. in the series of 2- or 4-halosubstituted esters, the interdependence between CL decay kinetics constants (k_{CL}) and pK_a values of the respective phenols was observed (Fig. 4).

The influence of surfactants on chemiluminescence

The cationic, zwitterionic and neutral surfactants (CTAC, DDAPS and Triton X-100, respectively) added to aqueous CL systems, containing XAEs, generally increase both the dynamics as well as efficiency of emission of light. The parameters quantitating that behavior are Δk_{CL} and $\Delta RCLE$, respectively and the relevant data is summarized in Table 3. The acceleration of CL kinetics decay for investigated XAEs obeys the order (an average values of Δk_{CL} are given in parentheses): DDAPS (1.5) > CTAC (1.1) > Triton X-100 (0.9). The general trend observed in all cases (CTAC, DDAPS, Triton X-100) is that the values of Δk_{CL} increase with the increase of inductive constants of substituents present in the benzene ring (σ_I = 0.76, 0.52, 0.47, 0.50 and 0.39 for NO_2, F, Cl, Br and I, respectively).[45] From the other hand, the enhancements of CL efficiency for the investigated XAEs are arranged in the following order (in parentheses average values of $\Delta RCLE$ are given): DDAPS (2.2) ≈ Triton X-100 (2.2) > CTAC (1.7). The most efficient CL systems among the studied ones such as **2,6-diF**/DDAPS or **2-F**/TritonX-100, express more than three-fold enhancement of

CL (Table 3, columns 6, 9) in comparison to the typical environment, in which the emission of XAEs is triggered (Table S4†, column 6, ESI).

As it was observed for similar systems, the dynamics and efficiency of CL is distinctly accelerated in the presence of cationic or zwitterionic surfactants, such as CTAC and DDAPS.[24,43] Such a bimolecular reactions can undergo micellar catalysis, based on the ability to bind various substrates and attract oppositely charged entities towards their surfaces.[44] In the context discussed here, the latter phenomenon is presumably manifested by the local increase in concentration of the hydroperoxide ions at the oppositely charged micellar surfaces and, resultantly – more efficient formation of the adequate hydroperoxide adducts (Scheme 2, **a**), that initiate the "light path" of reaction (Scheme 2, pathway I). In contrast to the above, when using a neutral surfactant such as Triton X-100, no impact (or even a slight decrease) of the rate of CL was detected – which is consistent with the previous observations made on similar CL systems.[24,43] However, clear influence of the above neutral detergent on the efficiency of emission is observed in the case of considered herein group of compounds, which differentiates the behavior of XAEs from other acridinium esters (labels and their conjugates) investigated in this context.[24] It should be noted, that the chemiluminogenic adduct, from which the transformations starts, is neutral in the case of the molecular systems studied here (Scheme 2, **a**). Taking into account the structure of Triton X-100, similar to the polyethylene glycols (PEGs), one can expect the occurrence of specific intermolecular interactions of the latter intermediate (**a**) with this neutral detergent – such as hydrogen bondings and the hydrophobic interactions of the XAEs' aromatic ring systems with the micelles. The latter phenomenon can lead to the increased local concentration of the chemiluminogenic adduct, and – resultantly – an increase in emission efficiency ($\Delta RCLE$) and, at the same time, diminution of the reaction rate due to the involvement of **a** in the above mentioned interactions. Our further investigations of this interesting problems are in progress.

For the above discussed enhanced CL systems, we also established the limits of detection (*LOD*) and limits of quantification (*LOQ*) at the maximal detector's sensitivity (Table 3, columns 4, 7, 10). The above parameters, depending basically on the slope of the calibration graphs, the deviation of the measured points from the linear regression, and the number of measured points (eq. S1†, eq. S2†, ESI) are of great analytical importance.[46] The relationships used for the calculation of *LOD*/*LOQ* and the exemplary calibration graphs are presented in Fig. S3B† (ESI). Among the studied CL systems, the lowest values of *LOD*/*LOQ*

– falling at the level of 1.3–2.9×10^{-11} M for *LOD* and 2.1–4.8×10^{-11} M for *LOQ*, respectively – were obtained with the participation of **2,6-diF** and **2-NO_2** and a cationic surfactant CTAC.

The products secreted upon XAEs' chemiluminescence

The mixtures obtained after the completion of CL were immediately subjected to RP-HPLC analyses in order to reveal the type and population of the products. An exemplary chromatogram for the reaction mixtures is presented in Fig. S4† (ESI). The products found after CL of XAEs were always 10-methyl-9-acridinone (NMAON) (the most intense signal at 254 nm and 268 nm), 10-methylacridinium-9-carboxylic acid (NMACA) and the substituted phenol (RPhOH). The above signals were attributed by the comparison of their retention times (R_T) with the ones found for previously prepared standard substances (NMAON, NMACA)[17] or purchased (RPhOHs) as reference compounds. The other trace signals observed in the chromatograms were analytically insignificant and they were therefore not quantified. The data concerning the content of NMACA in post-CL mixtures, assayed for compounds **2,6-diF**, **2,6-diCl**, **2,6-diBr** and **2,6-diI** in standard CL conditions is summarized in Table 4 (column 2). As the emissions from the above haloesters represent flash–type decays, the content of the acid, assessed with the use of calibration graphs (Figure S4B†, ESI), is generally low and falls in the range of ca. 0.2–2.7 mol%. The results indicate that, in the group of investigated compounds, the content of acid in the reaction mixtures does not clearly depend on the type of substituent. Interdependences were observed among the pseudo-first order kinetic constants of alkaline hydrolysis of 2,6-disubstituted XAEs at pH = 12 (k_{OH}) and the size parameters, characterizing the substitutents (halogen atoms) (Table 4, columns 4, 5). According to that, k_{OH} take the values, which are in an approximate relation of 1.0, 0.2 and 0.06 for **2,6-diF**, **2,6-diCl** and **2,6-diBr**, respectively.

The ESI-MS mass spectra, obtained for the mixtures under CL or just after the completion of CL reaction with the participation of selected XAEs in an alkaline aqueous environment are given in Figure 5. It can be seen that, instead of the cations observed in the MALDI-TOF experiments (Fig. S2† (ESI)), signals arise from the charged products of the oxidative decomposition of the acridinium salts, i.e. m/z ≈ 210 (NMAON) and m/z ≈ 238 (NMACA). The relative abundance of the latter cation is traceable in the case of the investigated 2,6-disubtituted salts (**2,6-diF** and **2,6-diI**) – which underlines the statements drawn from the above-discussed RP-HPLC experiments. It should also be noted that, among the cations detected, an acridinium fragment corresponding to the detachment of the

substituted phenoxy fragment from the parent acridinium cation (m/z ≈ 221 (M−1)) has a relative abundance at the level of several percents (ca. 15 and 27% for **2,6-diF** and **2,6-diI**, respectively).

Conclusions

Newly synthesized acridinium esters containing substituents of various electronic and steric characters such as halogens, CF_3, NO_2, and OCH_3 located at the ortho-, para- or meta-positions of the benzene ring (XAEs, Scheme 1) were subjected to a comprehensive theoretical and physicochemical investigation. The main tasks of this work included the assessment of the mechanism of their chemiluminogenic oxidation in basic protic solvents, as well as a thorough evaluation of their emission abilities in various environments.

By applying computational methods, based on the Density Functional Theory (DFT), we have proposed a number of possible steps concerning the transformations of XAEs in an aqueous alkaline environment, with the participation of ions such as OH^- and OOH^-. The latter may compete for the electron-deficient acridinium C(9) atom in the initial steps of the XAE transformations. In general, three concurrent reaction pathways have been proposed. Pathway one (blue arrows, Scheme 2) comprises the "light way" of XAE oxidation, involving 1.7–2.4% percent of the reaction energy released upon the transformation regards to experimentally obtained values of quantum yields (QY, Table S4† (ESI)). As stated before,[22,33] CL of the acridinium cations starts from the attack of OOH^- on the electron-deficient C(9).[22,33] Interestingly, the acridane-type adduct thus formed undergoes further transformations via two slightly different channels – as suggest thermodynamic features of the investigated systems and the values of the p_z LUMO orbital at the acridinium C(9) atom, reflecting susceptibility of XAEs for the attack of a nucleophile. The two alternative pathways seem to be dependent on the character of "leaving group", being detached upon the reaction. The fluorinated esters such as **2-F**, **2-CF_3** and 2-methoxy (**2-OCH_3**) are characterized by the occurrence of the cyclic dioxethane anionic form (**b**, Scheme 2) at the "bottleneck" stage of the pathway and behave similarly to the previously investigated alkyl-acridinium esters.[22] The second pathway includes the formation of the cyclic dioxetanone – the structure suggested in the literature as the crucial intermediate of the acridinium ester CL transformations – although up to date there is no clear experimental evidence demonstrating its occurrence. Both cyclic intermediates make an immediate, high-energetic precursors of the electronically excited

molecules of 10-methyl-9-acridinone (NMAON), the final emitter in all the CL systems based on acridinium salts.[17,47]

The other two general pathways are considered as "dark" – making concurrent reaction channels to the above-discussed "light way". The latter two pathways denote a "pseudabase way" (pathway two, red arrows, Scheme 2) – ending with the formation of NMAON in an electronic ground state and a "hydrolytic way" (pathway three, green arrows, Scheme 2) – ending with the formation of 10-methylacridine-9-carboxylic acid (NMACA) in the ground electronic state. Each of the three pathways ends up with chemically stable products, which were observed experimentally using chromatographic (RP-HPLC) and mass spectrometry (ESI-MS) techniques. Their populations in the reaction mixtures upon the completion of CL reflects the character of the substituents present in the benzene ring of the XAEs. However, at this stage of the research, we were unable to observe any of the high-energetic reaction intermediates revealed by computations.

The measurements of the XAEs' time profiles enabled us to assess the CL decay constants (k_{CL}) and the Relative Chemiluminescence Efficiencies (*RCLE*) in various environments (Table S4†, ESI). To do so, we tested XAEs in aqueous or methanolic solutions, containing various bases and additives such as sodium hydroxide, tetrabutylammonium hydroxide and 1,8-diazabicyclo[5.4.0]undec-7-ene, as well as cationic, zwitterionic or neutral surfactants such as cetyltriethylammonium chloride, dimethyldodecylammoniopropane sulfonate and Triton X-100. All the XAEs, except **2-OCH$_3$** (the only chemiluminogenic salt in the studied group, bearing an electron-donor substituent) emit a flash-type blue radiation (ca. 450−455 nm) in aqueous or methanolic solutions, completed within 1–2 seconds, regardless of the steric hindrance caused by spatial atoms (Br, I) attached at the *ortho* positions of the lateral benzene ring of XAEs. In all cases the aqueous triggering reagents, including quaternary ammonium base (H_2O_2 + TBAOH) allowed to obtain 2–20% higher *RCLE* if compared to standard (H_2O_2 + NaOH) or other triggers (H_2O_2 + DBU; H_2O_2+ TBAOH in CH_3OH) (Figure 2B). A distinct decrease in the XAEs' *RCLE* values upon lowering of the aqueous environment's pH was observed (Fig. 3A). The effect was most pronounced in the case of the **2-OCH$_3$** (deactivated by the substituent for the nucleophilic attack) while it is less pronounced in the cases where the esters bear substituents of distinct negative inductive effect, such as **2-NO$_2$** or **2,6-diF** (retaining ca. 50% of emission ability at pH = 8). Among the compounds investigated, **2-OCH$_3$**, **4-Br** and **3-F** can be recommended as fragments of CL labels due to their high usefulness at pH = 12 (the product

of relative efficiency and stability at given pH), while compounds **2,6-diF**, **2-NO_2**, expressing high usefulness at pH = 8, are interesting reagents in applications where high alkalinity of the environment makes a limitation (Fig. 3B).

The screening of the influence of surfactants on the emission ability and kinetics enabled us to select the CL systems of optimal performance – some of them, containing pairs of reagents such as **2,6-diF**/DDAPS or **2-F**/Triton X-100, express more than 3 times higher efficiency compared to the emission in typical aqueous environments with no enhancers (H_2O_2/NaOH).

The amounts of the acid (NMACA), the product of XAEs' alkaline hydrolysis, detected in the post-CL reaction mixtures, are traceable (below 2.5 mol%). The latter presumably arise from the fact, that the values of alkaline hydrolysis constants (k_{OH}) are 2–3 orders of magnitude lower than the respective constants of CL decay (k_{CL}), as revealed among acridinium 2,6-dihaloesters (Table 3 and S3† (ESI)). Other experiments revealed, that the alkaline hydrolysis at pH =12 of sterically hindered compounds, such as **2,6-diBr,** occurs ca. 17 times slower than the hydrolysis of the compound **2,6-diF**, as indicated by values of k_{OH} (Table 4).

We hope the present work will enhance the knowledge on the mechanism of oxidative transformations and physicochemistry of the acridinium esters bearing various atoms or group of atoms in their phenoxy moieties, involved in generation of light. Knowledge on their CL properties in various liquid environments is useful in the rational design of new luminogenic labels and indicators to be employed in ultrasensitive biomedical and/or environmental analytics.

Experimental

Computations

Unconstrained geometry optimizations of isolated molecules (Scheme 1) were carried out, at the DFT level of theory,[48] using the B3LYP functional[49] and 6-31G** basis sets[50] implemented in the GAUSSIAN 09 program package.[51] After completion of each optimization, the Hessian (second derivatives of the energy as a function of the nuclear coordinates) was calculated to assess whether stationary structures had been obtained.[48] The harmonic vibrational frequencies were then derived from the numerical values of these second derivatives and used to obtain the enthalpy and Gibbs' free energy contributions at 298.15 K and standard pressure (^{o}) with the aid of a built-in computational program of statistical thermodynamics routines.[52] The solvent (water) effect with completed optimization of each

molecules was included in the DFT calculations at the level of the Polarized Continuum Model (PCM) (UAHF radii were used to obtain the molecular cavity).[53]

The enthalpies ($\Delta_{r,298}H^o$) and Gibbs' free energies (free energies in the case of DFT(PCM)) ($\Delta_{r,298}G^o$) of the reactions (r), as well as the enthalpies ($\Delta_{a,298}H^o$) and Gibbs' free energies (free energies in the case of DFT(PCM)) ($\Delta_{a,298}G^o$) of activation (a) indicated in Scheme 1 were calculated by following the basic rules of thermodynamics.[54] The rate constants ($_{298}k^o$) for the gaseous phase reactions were obtained by applying the equation

$$_{298}k^o = \frac{RT}{Nh}\exp[-\Delta_{a,298}G^o/(RT)] \quad (1)$$

resulting from transition state theory, and the reaction completion time ($_{298}\tau_{99}$) from the formula

$$_{298}\tau_{99} = \ln 100/_{298}k^o \quad (2)$$

where R, T, N, and h denote the gas constant, temperature (298.15 K), Avogadro number, and Planck's constant, respectively.[54]

Chemical identity of XAEs and spectroscopic analyses of XAEs

9-[(Phenoxy)carbonyl]-10-methylacridinium triflates, substituted in the benzene ring (XAEs, Scheme 1), were synthesized by adopting the procedures reported before.[25-32] The structures and IUPAC names of the compounds obtained for this work are depicted in Scheme 1. The detailed data, concerning chemical synthesis and identity (retention times (RP-HPLC), melting points, elemental analysis) of the compounds investigated in this work are given in ESI†.

XAEs were subjected to structural analyses with the aid of nuclear magnetic spectroscopy (^{1}H NMR, ^{13}C NMR, ^{1}H–^{1}H COSY) and MALDI-TOF (Matrix Assisted Laser Desorption Ionization Time of Flight as well as ESI (Electrospray Ionization) mass spectrometry (MS) techniques. The nuclear magnetic resonance spectra (^{1}H NMR, ^{13}C NMR) were registered in CD_3CN or DMSO-d_6 (300 K) using a *Unity 500 Plus* spectrometer (*Varian*) with a 5 mm PFG probe. In some cases, the two-dimensional ^{1}H–^{1}H COSY and HETCOR techniques were employed for the unequivocal assignment of signals (). The experimental results were compared with the simulated spectra generated with the aid of ^{1}H NMR ACD package.[55] The masses of parent cations involved in XAEs were established using *VG Trio-3* triple quadrupole mass spectrometer (Masslab, Altrincham, UK) with 2,5-dihydroxybenzoic acid (DHB) as a matrix. Mass spectra were acquired in the positive polarity mode with the 100–700 m/z range of scan. The laser was set to 125 shots and the TOF detector was set to

linear mode with a 20 kV difference of potentials. The molecular ions recorded, together with basic fragmental ions, are summarized in Table S1† (ESI). In the case of selected XAEs, ESI-MS spectra were registered for the post-CL reaction mixtures, using a *Bruker-Esquire* LC Electrospray Ionisation Mass detector (*Bruker-Daltonic* GmbH, Germany). The mass spectra were acquired in the positive ion mode in the scan range of m/z 100−600. Capillary exit, trap drive and skimmer voltages were set to 81.9 V, 27.6 V and 15 V, respectively.

Measurement of chemiluminescence

Investigations of XAEs' (Scheme 1) chemiluminescence were conducted in two fashions using a *Fluoroskan Ascent FL* plate luminometer (*Labsystems-Thermo*). To compare the kinetics and efficiency of the emission, the equipment was operated at moderate sensitivity (photomultiplier tube (PMT) voltage = 340 mV) and the resolution of 20 ms/point. To record the kinetic profiles, the compounds were dissolved in anhydrous acetonitrile (*Aldrich*) to obtain a concentration of 5.0 mM. Portions of such prepared stock solutions were diluted with 1 mM aqueous HCl to obtain a concentration of 4×10^{-5} M and 200 µl aliquots of the latter were serially dispensed (n = 5) over the 96-well white polystyrene plate (*Cliniplate*). Next, portions of H_2O_2 solution (100 µl, 0.06%) in 0.01 M HNO_3 were added to each well and the plate was shaken for 30 seconds. CL was triggered by adding 100 µl of NaOH solution (0.2 M) and collecting the light output over 2-minute periods at 298 K. The above experiments were repeated in the same manner using other bases (c = 0.2 M): tetrabutylammonium hydroxide (TBAOH) and 1,8-diazabicyclo[5.4.0]undek-7-ene (DBU). Values of CL decay constants (k_{CL}) were calculated as negative values of the slopes of $\ln (I_{CL}/I_{CL}^{0}) = f$(time (s)) dependences.

To measure the efficiency of CL, the above acidic solutions of XAEs were serially diluted with 1 mM HCl to obtain solutions in a range of concentration $4\times10^{-5} - 4\times10^{-8}$ M and were treated as described above. The integral light outputs were collected by calculating the area under each kinetic profile, applying the implemented *Ascent FL* software. The calibration graphs were obtained upon linearization of the following relationship: Area under CL profile (A, RLU^2) = f(XAE concentration (M)). The values of emission efficiency for each CL system were obtained as the slopes of the linear calibration graphs and normalized to the highest value (*RCLE*).

To compare the CL efficiencies of XAEs at various pH, 50 µl aliquots of their acidic solutions (c = 4×10^{-5} M) were added to a wells of the white plate (n = 5). Next, a 50 µl

portion of 0.12% w/w H_2O_2 in 0.01 M HNO_3 was added to each well and the plate was shaken for 30 seconds. CL was triggered by adding 200 µl Britton-Robinson buffer (pH = 8.0, 10.0, 12.0) and the integral light outputs (A) were collected over 2-minute periods. The CL efficiency for XAEs were calculated from the formula:

CL efficiency = 100% × A, (given pH)/A for the most efficient system.

To assess the stability of XAEs in alkaline environments, XAE stock solutions were diluted with Britton Robinson buffer (pH = 8.0), to reach a final concentration of salt of 4×10^{-5} M. The solutions were then incubated at 298 K for 30 minutes and 200 µl aliquots of the ones were added to each well of the plate (n = 5), followed by the addition of 100 µl of 0.06 % H_2O_2 in 0.125 M HNO_3 (to obtain pH = 3.0–3.5) and 30-seconds shaking of the mixtures. To trigger the emission, 100 µl of NaOH (0.3 M) was added (final pH = 12) and the light outputs were integrated over 1 minute periods. The stability of XAEs, regarded as the preserved initial activity, were calculated from the following equation:

Stability = 100% × A (t = 30 min. incubation) / A (t = 0, no incubation).

A second type of CL experiments were performed at the maximal sensitivity of the apparatus (PMT voltage = 1000 mV) for selected XAEs in the presence of various surfactants: cetyltrimethylammonium chloride (CTAC), dimethyldodecylammoniumpropane sulfonate (DDAPS) and Triton X-100. The acridinium salts were serially dissolved in 1 mM HCl to obtain a series of solutions of the concentrations in the range of 5.0×10^{-11} – 2.5×10^{-9} M. The solutions of surfactants (24 mM of CTAC or DDAPS and 60 mM of Triton X-100) were optimized and prepared in the oxidizing solution (0.01 M HNO_3 containing 0.06% H_2O_2). 100 µl aliquots of XAE solutions were distributed over a 96-well, white polystyrene plate (n = 5), followed by the addition of 50 µl of the solution of oxidant containing each of the above surfactant. CL was triggered by the addition of 50 µl of 0.2 M KOH to each well. Temporary intensities of CL (I_{CL}, RLU) were collected every 20 ms until the reactions were complete (up to 5 seconds). For comparison, the measurements were taken under the same conditions with no surfactants. The changes of the values of CL decay kinetic constants (Δk_{CL}) and emission efficiencies ($\Delta RCLE$) were calculated as the ratio of the value obtained under experiments carried out in the presence of a surfactant and the adequate value obtained with no surfactant (Table 3).

Products of XAEs' chemiluminescence

The products of CL were assayed directly after completion of the emission of light with the aid of a *Waters* chromatographic system (see ESI† Section). For these experiments, the column employed was a 150 × 4.60 C6 Phenyl 110, 5 μm (*Gemini, Phenomenex*) and the mobile phase consisted of 60%/40% v/v acetonitrile/phosphate buffer (2 mM Na_2HPO_4 + $NaHPO_4$, pH = 3.5). The emission of XAEs was triggered in Eppendorf vials, by mixing 20 μL of XAE (5 mM solution in anhydrous acetonitrile) with 50 μl of H_2O_2 in 0.1 M HNO_3, followed by the addition of 0.2 M aqueous NaOH (50 μL). After completion of the emission, the mixtures were acidified with a drop of H_3PO_4 and immediately subjected to chromatographic analyses (absorption detection at 254 and 268 nm). Post-CL reaction products were identified by comparison of their retention times (R_T) and signal intensities (A) with the analogous parameters obtained for standard substances − namely 10-metyl-9-acridinone (NMAON), 10-methylacridinium-9-carboxylic acid (NMACA) and the respective phenols (RPhOHs): 2,6-difluorophenol, 2,6-dichlorophenol, 2,6-dibromophenol and 2,6-diiodophenol. Calibration graphs prepared for NMAON and NMACA enabled the assessment of the content of the latter product in the post-CL reaction mixtures (Table 4, Fig. S4†).

To assess the pseudo-first order kinetic constants of alkaline hydrolysis for selected XAEs (k_{OH}, Table 4), the XAEs were dissolved in phosphate buffer (pH = 12, c_{XAE} = 1.0–1.5 mM) and were incubated at 298 K up to 5 min. To stop the reaction after a certain time, 200 μl of each of the above mixtures were treated with 10 μl solution of TFA/mobile phase (1/3 v/v) to obtain final pH = 3. Hydrolysis constants (k_{OH}) were established, using the above-mentioned *Waters* HPLC system (mobile phase: acetonitrile/0.1% TFA_{aq}= 1/1 v/v; stationary phase: *Waters Symmetry* C_8, 4.6 × 250 mm, 5 μm) with the UV-absorption detector set at 256 nm. Chromatographic runs were recorded after specified reaction times (20–200 s, n = 3) and the areas under the NMAON and NMACA signals were calculated using built-in *Empower™* software. The values of k_{OH} were established graphically, using a linear calibration charts, assuming c_0 values as the initial concentration of XAE in the mixture and the c_t values as the temporary concentration of the hydrolysis product (NMACA), established according to the areas under the signal (Figure S5† (ESI)).

Acknowledgments. This work was financed by the State Funds for Scientific Research through grant No. N N204 375740 (contract No. 3757/B/H03/2011/40) for the period

2010−2013 and by the National Scientific Center (NCN) through grant No. UMO-2012/05/B/ST5/01680 for the period 2013–2016. B.Z. acknowledges financial support from the European Social Fund within the project "The development program of the University of Gdansk in areas of Europe 2020 (UG 2020)". Calculations were carried out on the computers of the Tri-City Academic Network Computer Centre (TASK) and the Wroclaw Centre for Networking and Supercomputing (WCSS) (grant no. 215). The authors would like to thank Dr Anna Białk-Bielińska and DSc Marek Gołębiewski for recording the mass spectra. We are greatly indebted to Dr Dorota Zarzeczańska for her contribution to the pH measurements and Mrs Kinga Zelewska for her contribution to the preparation of samples for spectroscopic analyses.

References

1 I. Weeks, I. Beheshti, F. McCapra, A. K. Campbell and J. S. Woodhead, *Clin. Chem*., 1983, **29**, 1474–1479.

2 G. Zomer and J. F.C. Stavenuiter, *Anal. Chim. Acta*, 1989, **227**, 11–19.

3 K. Nakashima, *Kirk-Othmer Encyklopedia of Chemical Technology*, vol. 5, p. 840–863, John Wiley & Sons 2003. Accessed at: http://www.scribd.com/doc/30106884/Chemiluminescence-Analytical-Applicatios.

4 Y. Ando, K. Niwa, N. Yamada, T. Irie, T. Enomoto, H. Kubota, Y. Ohmiya and H. Akiyama, *Photochem. Photobiol*., 2007, **83**, 1205–1210.

5 A. Roda, M. Guardigli, E. Michelini, M. Mirasoli and P. Pasini, *Anal. Chem*., 2003, **1**, 462A–470A.

6 G. Zomer, J. F. C. Stavenuiter, R. H. Van den Berg and E. H. J. M. Jansen, *Pract. Spectrosc.*, 1991, **12**, 505–521.

7 G. W. Miller, C. A. Morgan, D. J. Kieber, D. W. King, J. A. Snow, B. G. Heikes, K. Mopper and J. J. Kiddle, *Mar. Chem*., 2005, **97**, 4–13.

8 K. Krzymiński, A.D. Roshal, O.P. Synchykova, B.P. Sandomierski, "The method of determining of antioxidant or oxidizing activity of organic extracts based on chemiluminescence of acridinium esters", Patent No. P 381 661 granted by the Polish Patent Office on 22.09.2011.

9 D. W. King, W. J. Cooper, S. A. Rusak, B. M. Peake, J. J. Kiddle, D. W. O'Sullivan, M. L. Melamed, C. R. Morgan and S. M. Theberge, *Anal. Chem.*, 2007, **79**, 4169–4176.

10 M. Adamczyk, P. G. Mattingly, *Luminescence Biotechnology. Instruments and Applications*, p. 77–101, K. Van Dyke, Ch. Van Dyke, K. Woodfork eds., Boca Raton, London-New York-Washington D.C., CRC Press 2002.

11 A. A. Waldrop III, J. Fellers and C. P. H. Vary, *Luminescence*, 2000, **15**, 169–182.

12 M. Adamczyk, D. D. Johnson, P. G. Mattingly, P. G. Moore and Y. Pan, *Bioconjugate Chem.*, 1998, **9**, 23−32.

13 L. J. Arnold Jr., P. W. Hammond, W. A. Wiese and N. C. Nelson, *Clin. Chem*., 1989, **35**, 1588–1594.

14 A. Fan, Z. Cao, H. Li, M. Kai and J. Lu, *Anal. Sci*., 2009, **25**, 587–597.

15 R. C. Brown, Z. Li, A. J. Rutter, X. Mu, O. H. Weeks, K. Smith and I. Weeks, *Org. Biomol. Chem.*, 2009, **7**, 386–394.

16 K. A. Browne, D. D. Deheyn, G. A. El-Hiti, K. Smith and I. Weeks, *J. Am. Chem. Soc.*, 2011, **133**, 14637−14648.

17 K. Krzymiński, A. D. Roshal, B. Zadykowicz, A. Białk-Bielińska and A. Sieradzan, *J. Phys. Chem. A*, 2010, **114**, 10550−10562.

18 A. Natrajan, Q. Jiang, D. Sharpe and J. Costello, *High quantum yield acridinium compounds and their uses in improving assay sensitivity*, United States Patent No. US 7,309,615B2, publ. date: Dec. 12, 2007.

19 R. Renotte, G. Sarlet, L. Thunus and R. Lejeune, *Luminescence*, 2000, **15**, 311–320.

20 A. Natrajan, Q. Jiang and D. Sharpe, *Stable acridinium esters with fast light emission*. United States Patent Application Publication, US 2010/0099077 A1, publ. date: Apr. 22, 2010.

21 A. Natrajan, D. Sharpe, J. Costello and Q. Jiang, *Anal. Biochem*., 2010, **406**, 204–213.

22 K. Krzymiński, A. Ożóg, P. Malecha, A. D. Roshal, A. Wróblewska, B. Zadykowicz and J. Błażejowski, *J. Org. Chem*., 2011, **76**, 1072−1085.

23 *Acridinium Protein Labeling Kit* (Catalog No. 200201), *Cayman Chemical Company*, Ann Arbor, MI, USA. Available at: http://www.caymanchem.com/pdfs/200201.pdf (visited 11/2014).

24 A. Natrajan, D. Sharpe and D. Wen, *Org. Biomol. Chem.*, 2011, **9**, 5092−5103.

25 A. Sikorski, K. Krzymiński, A. Konitz and J. Błażejowski, *Acta Crystallogr. Sect. C*, 2005, **61**, o227–o230.

26 A. Sikorski, K. Krzymiński, A. Niziołek and J. Błażejowski, *Acta Crystallogr. Sect. C*, 2005, **61**, o690–o694.

27 A. Sikorski, K. Krzymiński, A. Konitz and J. Błażejowski, *Acta Crystallogr. Sect. E*, 2005, **61**, o2131–o2133.

28 A. Sikorski, A. Niziołek K. Krzymiński, T. Lis and J. Błażejowski, *Acta Crystallogr. Sect. E*, 2008, **64**, o372–o373.

29 D. Trzybiński, K. Krzymiński, A. Sikorski and J. Błażejowski, *Acta Crystallogr. Sect. E*, 2010, **66**, o1313–o1314.

30 D. Trzybiński, K. Krzymiński and J. Błażejowski, *Acta Crystalogr. Sect. E*, 2010, **66**, o2771−o2772.

31 D. Trzybiński, A. Ożóg, K. Krzymiński and J. Błażejowski, *Acta Crytallogr. Sect. E*, 2012, **67**, o3205–o3206.

32 B. Zadykowicz, K. Krzymiński, P. Storoniak and J. Błażejowski, *J. Therm. Anal. Calorim.*, 2010, **101**, 429–437.

33 J. Rak, P. Skurski and J. Błażejowski, *J. Org. Chem.*, 1999, **64**, 3002–3008.

34 I. Fleming, *Frontier Orbitals and Organic Chemical Reactions*; Wiley, London, New York, 1976.

35 A. Boużyk, L. Jóźwiak, A. Yu. Kolendo and J. Błażejowski, *J. Spectrochim. Acta A*, 2003, **59**, 543–558.

36 N. Sato, *Tetrahedron Letts.*, 1996, **47**, 8519–8522.

37 K. Krzymiński, P. Malecha, B. Zadykowicz, A. Wróblewska and J. Błażejowski, *Spectrochim. Acta A*, 2011, **78**, 401–409.

38 A. Natrajan, D. Sharpe and D. Wen, *Org. Biomol. Chem.*, 2012, **10**, 3432–3447.

39 K. Smith, J. J. Yang, Z. Li, I. Weeks and J. S. Woodhead, *J. Photochem. Photobiol. A: Chem.*, 2009, **203**, 72–79.

40 A. M. García-Campaña, W. R. G. Baeyens, X. R. Zhang, E. Smet, G. Van Der Weken, K. Nakashima, A. C. Calokerinos, *Biomed. Chromatogr.*, 2000, **14**, 166–172.

41 G. Goor, J. Glenneberg and S. Jacobi, Hydrogen Peroxide, in: *Ullmann's Encyclopedia of Industrial Chemistry*. *Ullmann's Encyclopedia of Industrial Chemistry*, Weinheim: Wiley-VCH, 2007.

42 F. McCapra, *Pure Appl. Chem.*, 1970, **24**, 611–629.

43 A. Natrajan, D. Sharpe and D. Wen, *Org. Biomol. Chem.*, 2012, **10**, 1883–1895.

44 Y. Wang, X. Huang, Y. Li, J. Wang and Y. Wang, *Colloids Surfs. A: Physicochem. Eng. Aspects*, 2009, **333**, 108–114.

45 C. Hansh and A. Leo, *Substituent Constants for Correlation Analysis in Chemistry and Biology*, Wiley Interscience, New York, 1979.

46 P. C. Meier and R. E. Zünd, *Statistical methods in analytical chemistry*, Wiley, New York, 2000.

47 M. W. Cass, E. Rapaport and E. H. White, *J. Am. Chem. Soc.*, 1972, **94**, 3168–3175.

48 J. K. Labanowski, *Density Functional Methods in Chemistry*, J. W. Andzelm (Ed.), Springer-Verlag, New York, 1991.

49 (a) A. D. Becke, *J. Chem. Phys.*, 1993, **98**, 1372–1377; (b) A. D. Becke, *J. Chem. Phys.*, 1993, **98**, 5648–5652; (c) C. Lee, W. Yang and R. G. Parr, *Phys. Rev. B*, 1988, **37**, 785–796.

50 (a) P. C. Hariharan and J. A. Pople, *Theor. Chim. Acta*, 1973, **28**, 213–222; (b) W. J. Hehre, L. Radom, P. v. R. Schleyer and J. A. Pople, *Ab Initio Molecular Orbital Theory*, Wiley, New York, 1986.

51 M. J. Frisch, G. W. Trucks, H. B. Schlegel, G. E. Scuseria, M. A. Robb, J. R. Cheeseman, G. Scalmani, V. Barone, B. Mennucci, G. A. Petersson, et. al., *Gaussian 09 (Revision D.01)*, Gaussian, Inc., Wallingford, CT, 2013.

52 M. J. S. Dewar and G. P. Ford, *J. Am. Chem. Soc.*, 1977, **99**, 7822–7829.

53 (a) J. Tomasi and M. Persico, *Chem. Rev.*, 1994, **94**, 2027–2094; (b) V. Barone, M. Cossi, B. Mennucci and J. Tomasi, *J. Chem. Phys.*, 1997, **107**, 3210–3221.

54 P. W. Atkins and J. de Paula, *Atkins' Physical Chemistry*, Oxford University Press, Oxford, 9th edn., 2009.

55 A. Williams, S. Bakulin and S. Golotvin, NMR Prediction Software, Advanced Chemistry Development, Toronto, 2001, http://www.acdlabs.com.

Table 1 Thermodynamic data of the elementary steps of the reactions of selected compounds with OOH^- and OH^- [a]

step no. (Scheme 2)	substituent	gaseous phase		aqueous phase	step no. (Scheme 1)	substituent	gaseous phase		aqueous phase
		$\Delta_{r,298}H^o$	$\Delta_{r,298}G^o$	$\Delta_{r,298}G^o$			$\Delta_{r,298}H^o$	$\Delta_{r,298}G^o$	$\Delta_{r,298}G^o$
I	**2-F**	–164.2	–151.3	–43.3	X	**2-F**	–0.1	–24.4	–34.4
	2-CF_3	–167.1	–153.2	–44.1		**2-CF_3**	–6.6	–30.9	–39.0
	2-NO_2	–166.0	–153.5	–44.7		**2-NO_2**	–13.9	–38.5	–47.6
	2-OCH_3	–162.8	–150.5	–43.0		**2-OCH_3**	2.3	–21.8	–30.9
	2,6-diBr	–165.4	–152.8	–44.2		**2,6-diBr**	–20.2	–44.2	–45.8
II	**2-F**	–190.2	–180.2	–63.1	XI	**2-F**	–70.3	–56.0	–15.7
	2-CF_3	–192.9	–182.0	–64.4		**2-CF_3**	–72.6	–58.0	–16.8
	2-NO_2	–191.4	–181.1	–64.9		**2-NO_2**	–75.3	–61.7	–21.1
	2-OCH_3	–188.9	–178.4	–62.7		**2-OCH_3**	–64.4	–50.9	–12.2
	2,6-diBr	–188.0	–178.5	–62.6		**2,6-diBr**	–66.7	–51.0	–14.2
III	**2-F**	–138.4	–125.5	–25.0	XII	**2-F**	24.7	10.2	–3.7
	2-CF_3	–142.0	–128.2	–26.0		**2-CF_3**	24.4	9.8	–8.4
	2-NO_2	–135.4	–123.3	–23.0		**2-NO_2**	15.8	1.9	–13.1
	2-OCH_3	–133.9	–121.0	–22.4		**2-OCH_3**	31.5	18.6	–2.7
	2,6-diBr	–138.3	–124.9	–25.0		**2,6-diBr**	8.4	–6.3	–18.7
IV	**2-F**	–156.6	–146.6	–36.7	XIII		–94.2	–116.3	–118.6
	2-OCH_3	–152.3	–142.1	–34.9	XIV	**2-F**	–103.1	–104.1	–58.7
V	**2-F**	–75.4	–78.0	–51.7		**2-CF_3**	–105.3	–106.9	–60.8
	2-CF_3	–86.4	–89.1	–58.8		**2-OCH_3**	–100.9	–102.2	–58.2
	2-NO_2	–96.3	–99.8	–68.4	XV	**2-F**	–88.4	–103.0	–82.9
	2-OCH_3	–67.2	–69.7	–46.9		**2-OCH_3**	–84.5	–99.1	–80.0
	2,6-diBr	–91.7	–94.8	–64.7	XVI	**2-F**	–66.3	–80.1	–51.6
VI	**2-F**	–77.2	–78.3	–40.4		**2-CF_3**	–74.5	–89.2	–57.9
	2-CF_3	–80.1	–81.9	–42.7		**2-NO_2**	–85.4	–99.6	–66.8
	2-OCH_3	–72.0	–72.6	–37.6		**2-OCH_3**	–59.5	–72.5	–47.1
VII	**2-F**	–93.6	–108.0	–117.7		**2,6-diBr**	–81.5	–95.4	–63.7
	2-CF_3	–95.7	–111.0	–117.8	XVII	**2-F**	–92.2	–105.8	–69.9
	2-OCH_3	–97.6	–112.0	–118.0		**2-CF_3**	–99.6	–114.2	–76.0
VIII	**2-F**	10.8	2.2	0.4		**2-NO_2**	–116.0	–129.7	–88.5
	2-CF_3	7.7	–0.3	–3.6		**2-OCH_3**	–88.4	–102.0	–67.6
	2-OCH_3	16.4	8.1	2.4		**2,6-diBr**	–108.6	–123.2	–82.8
IX	**2-F**	–68.0	–68.7	–33.2	XVIII		–93.7	–104.1	–106.2
	2-CF_3	–69.8	–71.4	–34.5					
	2-NO_2	–73.9	–75.4	–34.9					
	2-OCH_3	–63.5	–64.7	–32.3					
	2,6-diBr	–66.5	–67.4	–35.4					

[a] $\Delta_{r,298}H^o$ and $\Delta_{r,298}G^o$ respectively represent the enthalpy and Gibbs' free energy (gaseous phase) or free energy (aqueous phase) of the reaction corresponding to a given step number at temperature 298.15 K and standard pressure. All thermodynamic data are in kcal mol^{-1}.

Table 2 Kinetic characteristics of the elementary steps of the reaction of selected compounds with OOH^- and OH^- [a]

step no. (Scheme 2)	substituent	gaseous phase			aqueous phase
		$\Delta_{a,298}H^o$	$\Delta_{a,298}G^o$	${}_{298}k^o$ (${}_{298}\tau^o_{99}$)	$\Delta_{a,298}G^o$
VII	**2-F**	9.3	8.5	3.4×10^6 (1.4×10^{-6})	14.1
	2-CF_3	10.8	10.7	9.5×10^4 (4.8×10^{-5})	14.6
	2-OCH_3	8.2	8.6	3.3×10^6 (1.4×10^{-6})	12.6
X	**2-F**	8.5	7.7	3.4×10^6 (1.4×10^{-6})	14.1
	2-CF_3	8.2	7.1	4.1×10^7 (1.1×10^{-7})	8.2
	2-NO_2	7.7	6.5	9.8×10^7 (4.7×10^{-8})	6.6
	2-OCH_3	8.8	7.9	1.1×10^7 (4.3×10^{-7})	8.0
	2,6-diBr	2.0	2.8	5.4×10^{10} (8.5×10^{-11})	5.2
XIII		32.6	33.0	4.0×10^{-12} (1.1×10^{12})	26.2
XVIII		10.3	10.1	2.6×10^5 (1.8×10^{-5})	15.4

[a] $\Delta_{a,298}H^o$ and $\Delta_{a,298}G^o$ (both in kcal/mol) respectively represent the enthalpy and Gibbs' free energy (gaseous phase) or free energy (aqueous phase) of activation at temperature 298.15 K and standard pressure. ${}_{298}k^o$ (in s^{-1}) and ${}_{298}\tau^o_{99}$ (in s) (Eqs. (5) and (6)) respectively denote the rate constant and the time after which the reaction is 99% complete.

Table 3 Effects of surfactants on CL parameters for selected XAEs in alkaline aqueous environments. For details see Experimental section.

compound code	CTAC			DDAPS			Triton X-100		
	Δk_{CL}[1]	$\Delta(RCLE)$[2]	*LOD*/*LOQ*[3] $\times 10^{-11}$ M	Δk_{CL}	$\Delta(RCLE)$	*LOD*/*LOQ* $\times 10^{-11}$ M	Δk_{CL}	$\Delta(RCLE)$	*LOD*/*LOQ* $\times 10^{-11}$ M
2-F	1.14	2.42	4.60/7.47	1.21	2.72	9.10/14.8	0.81	3.19	10.7/17.4
2-I	1.15	1.89	7.85/12.7	1.23	2.35	11.0/17.9	0.80	2.02	19.6/31.5
2-NO_2	1.24	2.12	2.93/4.78	1.37	2.36	7.24/11.8	1.00	2.45	6.36/10.2
2,6-diF	1.18	1.84	1.29/2.13	2.02	3.15	3.05/5.14	1.24	2.40	7.28/11.8
2,6-diCl	1.09	1.37	7.16/11.3	1.62	2.07	27.7/44.3	1.20	2.47	17.1/27.2
2,6-diBr	1.04	1.22	6.73/10.7	1.43	1.85	16.9/26.9	0.77	1.80	14.5/23.1
2,6-diI	1.10	1.26	15.0/24.0	1.79	1.16	14.3/22.9	0.49	0.93	17.3/27.5

Abbreviations:

[1]Δk_{CL} – denotes the change of CL decay kinetic constant value relative to the value obtained with no surfactant using standard triggering system (H_2O_2/NaOH) (see footnote 1 under Table S4† (ESI));

[2]$\Delta(RCLE)$ – denotes the change of integral CL intensity relative to the value obtained with no surfactant using standard triggering system (H_2O_2/NaOH) (also see Table S3† (ESI));

[3]*LOD*/*LOQ* – denotes the Limit Of Detection and the Limit Of Quantification, respectively.

Table 4 Chromatographically (RP-HPLC) assessed content of XAEs' alkaline hydrolysis product, 10-methylacridinium-9-carboxylic acid (NMACA) in the post-CL reaction mixtures. Pseudo-first order kinetics constants of XAEs' alkaline hydrolysis at pH = 12 (k_{OH}). For details see Experimental section.

Compound code	NMACA content[1] (mol%)	*CV* (%)	k_{OH}[2] ($\times 10^{-2}$ s^{-1})	Charton's size values (σ_V) / Taft size parameter (E_S) for adequate halogen atom [H]
2,6-diF	0.18	0.0	4.69	0.27 / –0.46
2,6-diCl	1.66	3.8	0.89	0.55 / –0.97
2,6-diBr	2.73	5.9	0.31	0.65 / –1.16
2,6-diI	1.07	4.9	–	0.78 / –1.40

Notes:
[1]Signals were identified by the comparison of their retention times with the ones assessed for the reference material. Values were established basing on the areas the under the signal of NMACA in relation to the calibration plots (Fig. S4† (ESI)).
[2]Values were obtained upon the linearization of ln $C_t/C_0 = f$(time) interdependences (n = 6–8, R^2 = 0.97–0.99) (Fig. S5† (ESI)).

Scheme 1 Structural formula and systematic names of investigated 10-methyl-9-(phenoxycarbonyl)acridinium trifluoromethanesulfonates (triflates) (XAEs) with the numbering system of C, N and O atoms given for the cation. Numbers of H atoms are the same as the C atoms to which the former are attached.

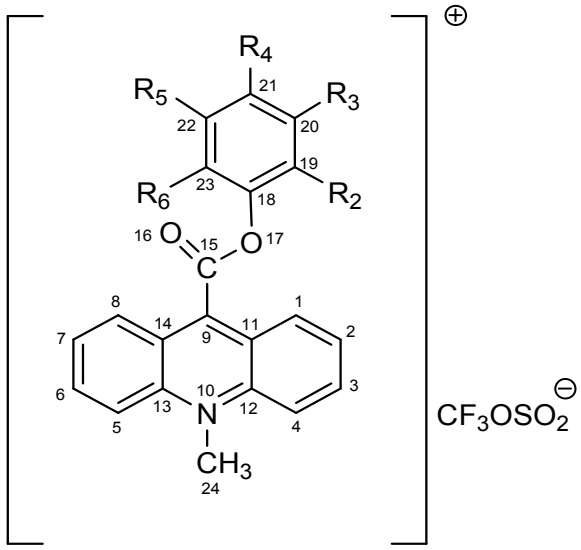

compound code	substituents in the benzene ring					name of the cation
	R_2	**R_3**	**R_4**	**R_5**	**R_6**	
2-F	F	H	H	H	H	9-[(2-fluorophenoxy)carbonyl]-10-methylacridinium
2-Cl	Cl	H	H	H	H	9-[(2-chlorophenoxy)carbonyl]-10-methylacridinium
2-Br	Br	H	H	H	H	9-[(2-bromophenoxy)carbonyl]-10-methylacridinium
2-I	I	H	H	H	H	9-[(2-iodophenoxy)carbonyl]-10-methylacridinium
2-CF_3	CF_3	H	H	H	H	10-methyl-9-{[2-(trifluoromethyl)phenoxy]carbonyl}acridinium
2-NO_2	NO_2	H	H	H	H	10-methyl-9-[(2-nitrophenoxy)carbonyl]acridinium
2-OCH_3	OCH_3	H	H	H	H	9-[(2-methoxyphenoxy)carbonyl]-10-methylacridinium
2,6-diF	F	H	H	H	F	9-[(2,6-difluorophenoxy)carbonyl]-10-methylacridinium
2,6-diCl	Cl	H	H	H	Cl	9-[(2,6-dichlorophenoxy)carbonyl]-10-methylacridinium
2,6-diBr	Br	H	H	H	Br	9-[(2,6-dibromophenoxy)carbonyl]-10-methylacridinium
2,6-diI	I	H	H	H	I	9-[(2,6-diiodophenoxy)carbonyl]-10-methylacridinium
3-F	H	F	H	H	H	9-[(3-fluorophenoxy)carbonyl]-10-methylacridinium
4-F	H	H	F	H	H	9-[(4-fluorophenoxy)carbonyl]-10-methylacridinium
4-Cl	H	H	Cl	H	H	9-[(4-chlorophenoxy)carbonyl]-10-methylacridinium
4-Br	H	H	Br	H	H	9-[(4-bromophenoxy)carbonyl]-10-methylacridinium

Scheme 2 Pathways of the Reactions of $MPCA^+$ with OOH^- and OH^- (pathway one (blue arrows), pathway two (red arrows) and pathway three (green arrows).

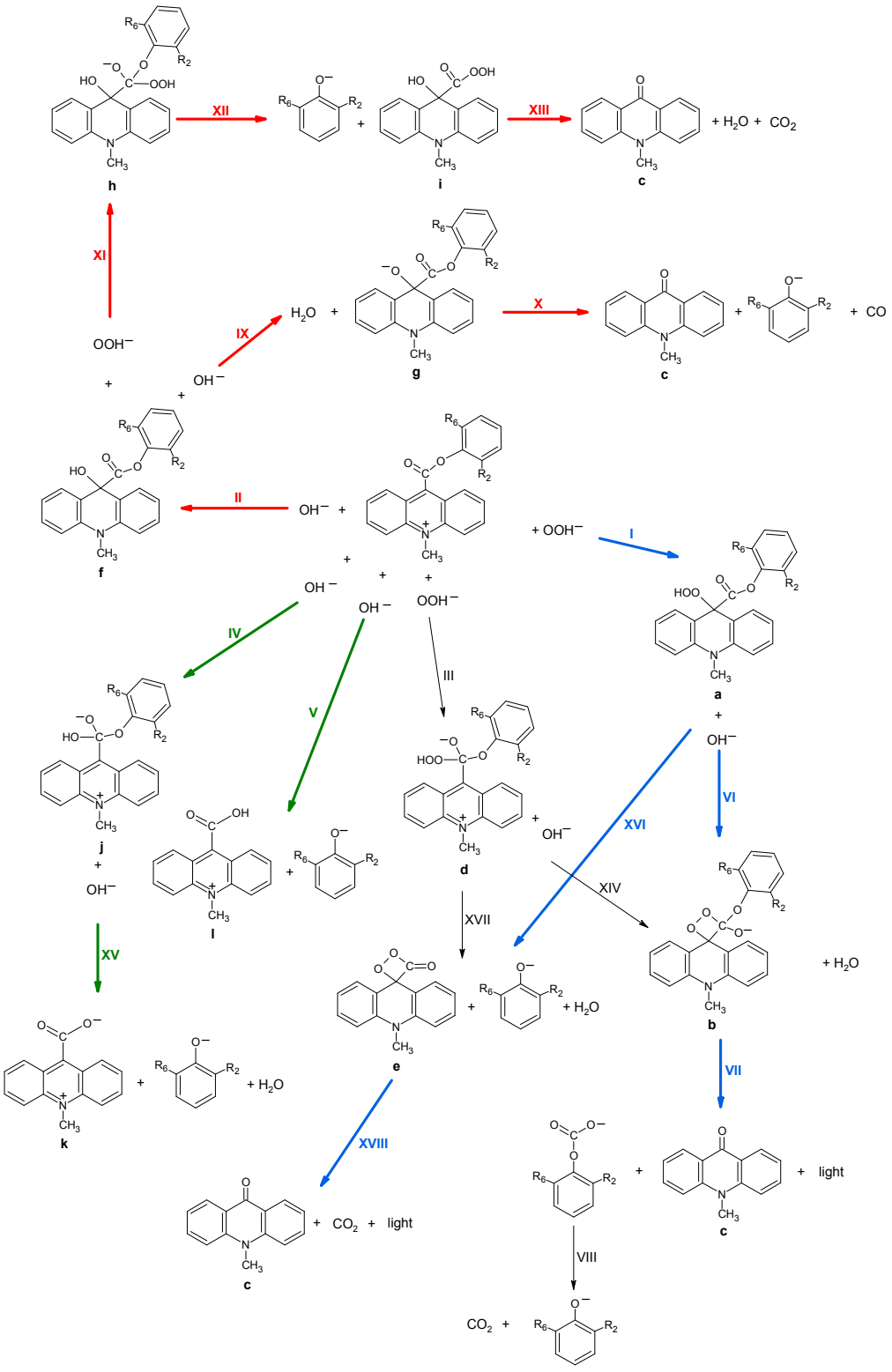

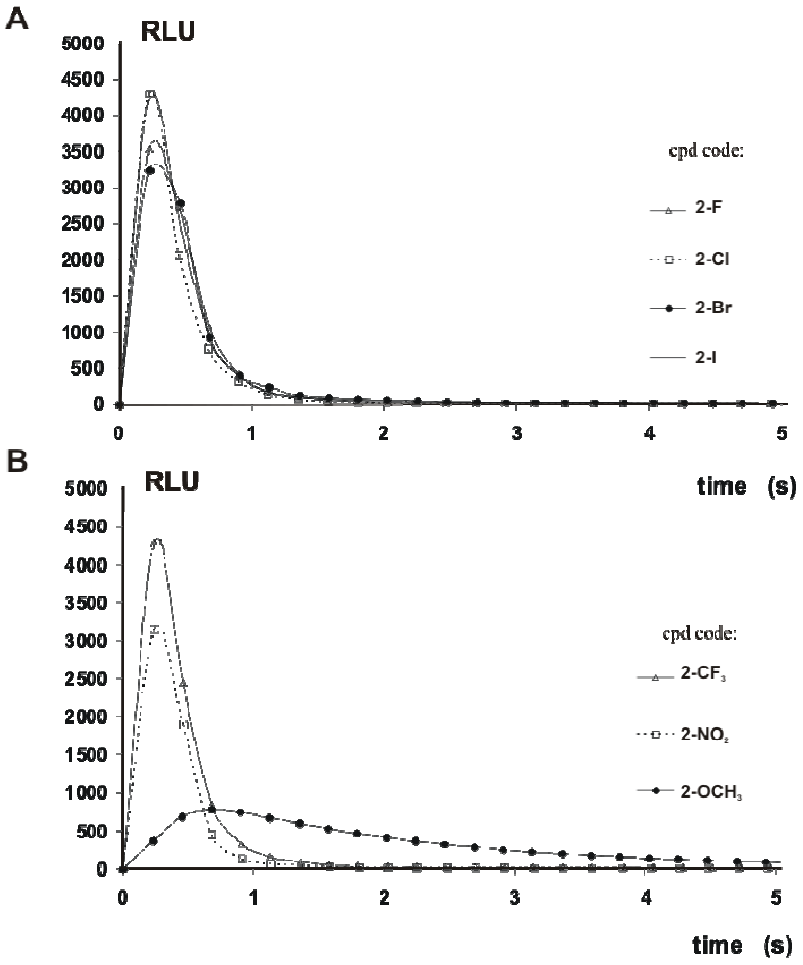

Fig. 1 Chemiluminescence profiles recorded for 2-substituted XAEs (Scheme 1) using a standard triggering system. A: CL profiles of 2-halosubstituted acidinium salts; B: CL profiles of other 2-substituted acridinium salts investigated. For details, see the Experimental section and note 1 to Table S4† (ESI).

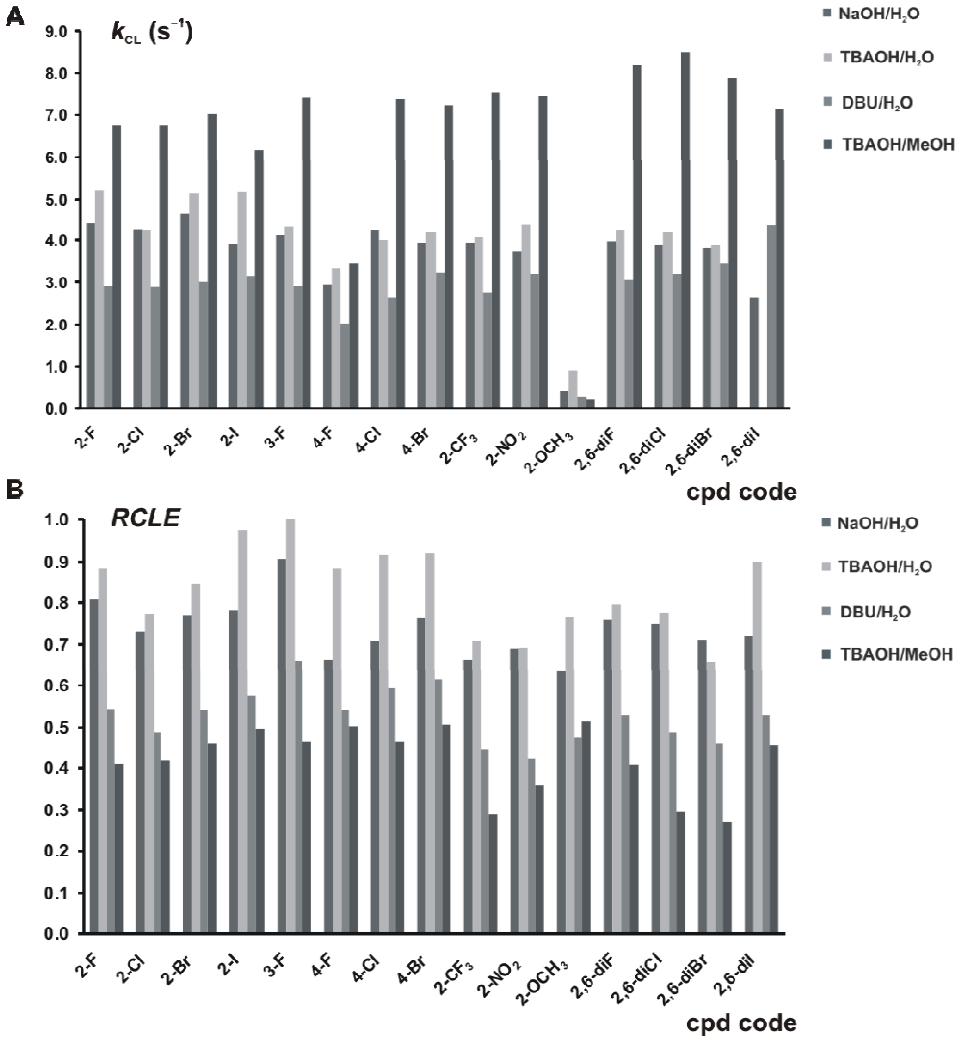

Fig. 2 CL parameters of XAEs (Scheme 1) in various environments. A: Pseudo-first order emission decay kinetic constants (k_{CL}); B: Relative CL efficiencies (*RCLE*, normalized) in various environments. The coefficients of variability (*CV*) fall in the range of 2–8%. Abbreviations: TBAOH – *tetra-n*-butylammonium hydroxide, DBU – 1,8-diazabicyclo[5.4.0]undec-7-ene; MeOH – methanol. For details, see the Experimental section and notes to Table S4† (ESI).

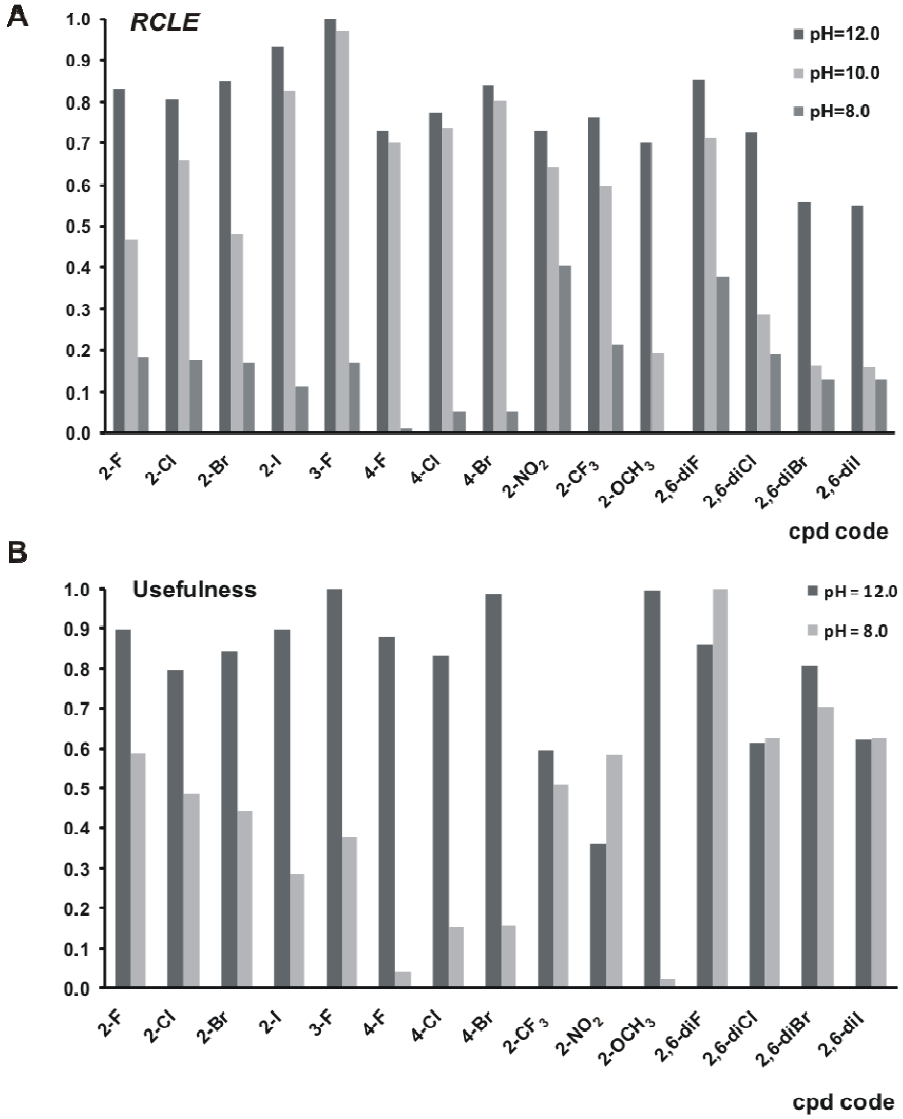

Fig. 3 CL parameters of XAEs (Scheme 1) in aqueous environments of different alkalinity. A: The dependence of *RCLE* (normalized to the highest value) on the pH. B: Usefulness (the product of stability at pH = 8.0 and the emission efficiency at given pH, normalized) in aqueous environments of different alkalinity. The coefficients of variability (CV) fall in the range of 2–8%. For details, see the Experimental section and notes to Table S4† (ESI).

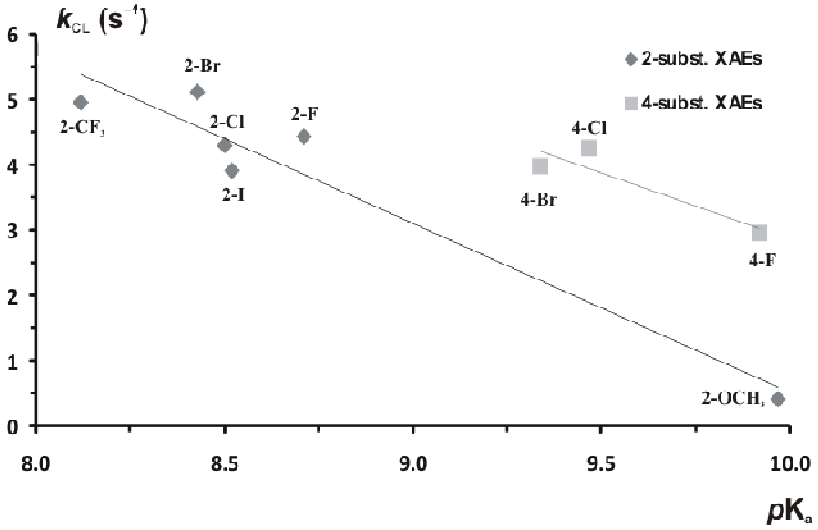

Fig. 4 The interdependencies between estimated ionization constants for respective phenols (pK_a) [ACD[55]] and the pseudo-first order constants of emission decay (k_{CL}) (Table S4†, column 2, ESI) for 2 or 4-substituted XAEs (Scheme 1). The lines correspond to the following equations: $k_{CL} = -2.593\text{p}K_a + 26.44$ (**2-subst. XAEs**), $k_{CL} = -2.045\text{p}K_a + 23.31$ (**4-subst. XAEs**). For details, see the Experimental section and note 1 to Table S4† (ESI).

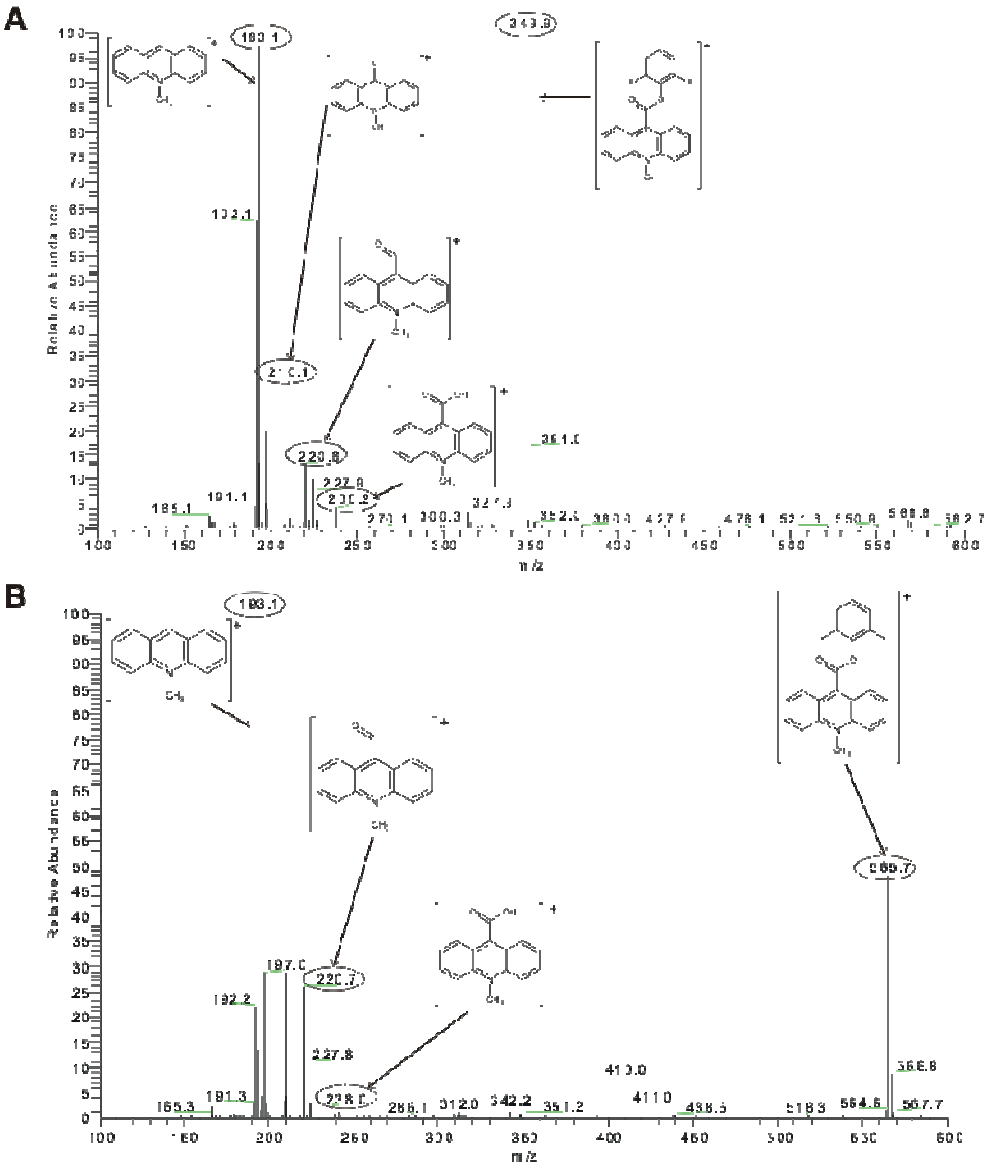

Fig. 5 ESI-MS spectra recorded in the positive ion regime for an exemplary XAEs (Scheme 1). A: 9-[(2,6-difluorophenoxy)carbonyl]-10-methylacridinium triflate (**2,6-diF**); B: 9-[(2,6-diiodophenoxy)carbonyl]-10-methylacridinium triflate (**2,6-diI**). For details, see the Experimental section.